SAND2014-18425R

Materials for Consideration in Standardized Canister Design Activities

Fuel Cycle Research & Development

Prepared for
U.S. Department of Energy
Used Fuel Disposition Program

C. Bryan, A. Ilgen, D. Enos,
S. Teich-McGoldrick and E. Hardin
Sandia National Laboratories
October 2, 2014

FCRD- NFST-2014-000642
SAND2014-xxxxxx

DISCLAIMER

This information was prepared as an account of work sponsored by an agency of the U.S. Government. Neither the U.S. Government nor any agency thereof, nor any of their employees, makes any warranty, expressed or implied, or assumes any legal liability or responsibility for the accuracy, completeness, or usefulness, of any information, apparatus, product, or process disclosed, or represents that its use would not infringe privately owned rights. References herein to any specific commercial product, process, or service by trade name, trade mark, manufacturer, or otherwise, does not necessarily constitute or imply its endorsement, recommendation, or favoring by the U.S. Government or any agency thereof. The views and opinions of authors expressed herein do not necessarily state or reflect those of the U.S. Government or any agency thereof.

Sandia National Laboratories is a multi-program laboratory managed and operated by Sandia Corporation, a wholly owned subsidiary of Lockheed Martin Corporation, for the U.S. Department of Energy's National Nuclear Security Administration under contract DE-AC04-94AL85000.

FCT Quality Assurance Program Document

Appendix E
FCT Document Cover Sheet

Name/Title of Deliverable/Milestone	Materials for Consideration in Standardized Canister Design Activities (FCRD- NFST-2014-000642)
Work Package Title and Number	**FT-14SN090403** Standardization Assessment - SNL
Work Package WBS Number	1.2.09.04
Milestone Number	**M4FT-14SN0904032**

Responsible Work Package Manager
Ernest Hardin (Name/Signature) — 03Oct2014 (Date Submitted)

Quality Rigor Level for Deliverable/Milestone	☒ QRL-3	☐ QRL-2	☐ QRL-1 ☐ Nuclear Data	☐ N/A*

This deliverable was prepared in accordance with Sandia National Laboratories
(Participant/National Laboratory Name)

QA program which meets the requirements of
☒ DOE Order 414.1 ☐ NQA-1-2000 ☐ Other: _____

This Deliverable was subjected to:
☒ Technical Review ☐ Peer Review

Technical Review (TR)
Review Documentation Provided
☐ Signed TR Report, or
TR Report No.: _____
☐ Signed TR Concurrence Sheet (attached), or
☒ Signature of TR Reviewer(s) below

Peer Review (PR)
Review Documentation Provided
☐ Signed PR Report, or
PR Report No.: _____
☐ Signed PR Concurrence Sheet (attached), or
☐ Signature of PR Reviewers below

Name and Signature of Reviewers

(Name/Signature)	(Date)
Yifeng Wang	10/2/2014

*Note: In some cases there may be a milestone where an item is being fabricated, maintenance is being performed on a facility, or a document is being issued through a formal document control process where it specifically calls out a formal review of the document. In these cases, documentation (e.g., inspection report, maintenance request, work planning package do
cumentation, or the documented review of the issued document through the document control process) of the completion of the activity along with the Document Cover Sheet is sufficient to demonstrate achieving the milestone. QRL for such milestones may also be marked N/A in the work package provided the work package clearly specifies the requirement to use the Document Cover Sheet and provide supporting documentation.

SUMMARY

This document identifies materials and material mitigation processes that might be used in new designs for standardized canisters for storage, transportation, and disposal of spent nuclear fuel. It also addresses potential corrosion issues with existing dual-purpose canisters (DPCs) that could be addressed in new canister designs. The major potential corrosion risk during storage is stress corrosion cracking of the weld regions on the 304 SS/316 SS canister shell due to deliquescence of chloride salts on the surface. Two approaches are proposed to alleviate this potential risk. First, the existing canister materials (304 and 316 SS) could be used, but the welds mitigated to relieve residual stresses and/or sensitization. Alternatively, more corrosion-resistant steels such as super-austenitic or duplex stainless steels, could be used. Experimental testing is needed to verify that these alternatives would successfully reduce the risk of stress corrosion cracking during fuel storage.

For disposal in a geologic repository, the canister will be enclosed in a corrosion-resistant or corrosion-allowance overpack that will provide barrier capability and mechanical strength. The canister shell will no longer have a barrier function and its containment integrity can be ignored. The basket and neutron absorbers within the canister have the important role of limiting the possibility of post-closure criticality. The time period for corrosion is much longer in the post-closure period, and one major unanswered question is whether the basket materials will corrode slowly enough to maintain structural integrity for at least 10,000 years. Whereas there is extensive literature on stainless steels, this evaluation recommends testing of 304 and 316 SS, and more corrosion-resistant steels such as super-austenitic, duplex, and super-duplex stainless steels, at repository-relevant physical and chemical conditions. Both general and localized corrosion testing methods would be used to establish corrosion rates and component lifetimes.

Finally, it is unlikely that the aluminum-based neutron absorber materials that are commonly used in existing DPCs would survive for 10,000 years in disposal environments, because the aluminum will act as a sacrificial anode for the steel. We recommend additional testing of borated and Gd-bearing stainless steels, to establish general and localized corrosion resistance in repository-relevant environmental conditions.

CONTENTS

FIGURES

TABLES

Acronyms

AISI/SAE	American Iron and Steel Institute/Society of Automotive Engineers
BCC	body-centered cubic
BCT	body-centered tetragonal
CFR	Code of Federal Regulations
CRIEPI	Central Research Institute of Electric Power Industry
DCPD	Direct Current Potential Drop
DPC	dual purpose cask
FCC	face-centered cubic
HAZ	heat affected zone
ISFSI	independent spent fuel storage installation
MCA	multiple crevice former assembly
NACE	National Association of Corrosion Engineers
NEUP	Nuclear Energy University Programs
NFST	Nuclear Fuel Storage and Transportation
NRC	U.S. Nuclear Regulatory Commission
SCC	stress corrosion cracking
SNF	spent nuclear fuel
SS	stainless steel
UFD	Used Fuel Disposition

MATERIALS FOR CONSIDERATION IN STANDARDIZED CANISTER DESIGN ACTIVITIES

1. INTRODUCTION

This report reviews possible materials for use in standardized canisters for the storage, transportation, and disposal of spent nuclear fuel (SNF) that would result in improved performance relative to existing dual-purpose canister (DPC) designs. For performance prior to disposal, the primary barrier function of the canister is to maintain isolation by resisting through-wall penetrations. The most important scenario for canister failure is by through-wall stress corrosion cracking (SCC) of the canister walls at welds and weld heat-affected zones, where recent material modeling indicates that through-wall tensile residual stresses may be present (NRC 2013). Current storage canisters, which are manufactured of austenitic stainless steels such as Types 304 and 316, are susceptible to SCC. Use of other, more corrosion-resistant metals and/or weld residual stress mitigation techniques are discussed here.

As per 10 CFR 72.236(m), final disposal must be considered in the design of interim storage casks. It is reasonable that waste isolation, the primary performance metric after disposal, will be provided by natural and engineered barriers, including a disposal overpack. The containment function of the disposal overpack is not assigned to the canister since this would eliminate the advantage of using a single canister design with specialized overpacks for storage, transportation, and disposal. For example, the disposal overpack could be designed for mechanical strength sufficient to resist crushing in a repository, with thick walls and increased weight, but this would negatively impact storage and transportation operations.

The disposal overpack will be designed to provide robust containment, either with a thick layer of corrosion-allowance material, or a thinner layer corrosion-resistant material supported by one or more additional layers of structural material. The fuel canister and its internals could provide additional structural strength, but the contribution is likely to be small relative to that of the overpack, and this function has been excluded for simplicity in other studies (see Hardin et al. 2013).

After breach of the waste package (overpack and canister shell) the main function of the fuel canister and its internals will be to mitigate the risk of nuclear criticality. This will occur in two ways: by maintaining the configuration of the fuel assemblies, and by maintaining the function of neutron absorbing elements (if any). As the overpack, canister, and basket corrode the structural integrity of the basket and assemblies will gradually degrade. Rearrangement of the fuel assemblies, along with flooding of the canister with ground water, could significantly increase reactivity. Degradation and displacement of neutron absorber materials in the basket could also significantly increase reactivity. These conditions could also substantially increase the uncertainty of neutronic configurations. Accordingly, the goals of this report are to identify materials for use in basket structures and neutron absorbing components, that can sustain their respective functions after canister flooding, for a nominal performance period of 10,000 years.

This analysis and test plan first discusses corrosion of materials for the canister shell and its internals during storage and disposal (Section 2). Chemical environments for canisters in storage and after geologic disposal are then presented (Section 3). Prospective materials are discussed (Section 4), and finally a suite of corrosion tests is proposed that would significantly reduce uncertainty as to the corrosion performance of these materials under repository-relevant conditions (Section 5).

2. MATERIAL CORROSION DURING STORAGE AND DISPOSAL

In order to determine what materials to consider for a standardized cask, a review of materials currently in use is provided here. Known corrosion issues are discussed, and the desired performance is described.

2.1 Canister shell

Current interim storage canisters for SNF are made of 304 or 316 SS. In the past, the carbon content of these has generally not been specified; current canisters may be, but are not required to be, low carbon steel, 304L or 316L (note that modern steels are largely dual certified—material sold as 304 or 316 SS meets the qualifications for 304L or 316L SS, respectively). Moreover, most of the canisters are welded canisters, and during manufacturing, no steps were made to mitigate the effects of the welds on the corrosion resistance of the metal. Welds have two major effects with respect to corrosion.

- They induce residual stresses in the weld and the adjacent heat-affected zone (HAZ). Residual stresses reduce the corrosion resistance of the metal, increasing pitting and general corrosion rates. Residual stresses, if sufficiently high, can also support SCC of the metal.
- Heating due to welding can cause the metal to become sensitized. Sensitization occurs when carbon and chromium in the steel diffuse to the grain boundaries and combines to form chrome-rich carbides. This results in a Cr-depleted selvage on the grains along the grain boundaries, which corrodes much more readily than the base metal. Grain boundary corrosion also helps support stress corrosion cracking. Note that the weld material itself cools from a molten state and is annealed; it does not become sensitized.

Concerns of the performance of existing stainless steel interim storage canisters are largely due to the potential for SCC due to deliquescence of salts that are deposited on the canister surface as outside air is convected through the overpack. 300 series stainless steels are known to susceptible to stress corrosion cracking in near-marine settings, where chloride-rich salts may be deposited on the surface and deliquesce to form a corrosive brine (Kain 1990). In combination with anticipated high weld residual stresses (NRC 2013) and potential sensitization in the HAZ, SCC may be possible. Several experimental studies (e.g., Nakayama 2006; Tani et al. 2009, 2010; Mintz et al. 2012; Prosek et al. 2009, 2014; NRC 2014) have observed SCC under conditions nominally typical of the surface of interim storage canisters stored at near-marine Independent Spent Fuel Storage Locations (ISFSIs).

To improve the corrosion properties of a standardized cask, two modifications that could be made. First, using the same 300-series steels, the weld effects could be reduced or eliminated through mitigations such as shot or laser peening or post-weld annealing. Second, different metals, more resistant to corrosion, could be used.

Corrosion Performance for Canister Shell After Disposal. As noted previously, it is assumed that the canister will be placed within an overpack prior to disposal, and the waste isolation and mechanical strength functions of the overall waste package are assigned to the overpack. Hence, corrosion performance of the canister shell after disposal would not be required, except that the material not interact galvanically with other components in the canister.

2.2 Basket materials

The basket within a SNF canister supports and maintains the waste assemblies and the neutron absorbers in a geometry that limits the potential for criticality. Canisters used currently for SNF storage have baskets that are made mostly of 304 SS, 316 SS, and/or other stainless steel types (and a few other materials such as aluminum and coated or plated low-alloy steel).

Corrosion Performance for Basket During Storage At loading, canisters are purged of moisture and filled with helium (or other inert gas), so that significant corrosion cannot occur internally. Even should a canister be breached, perhaps by SCC, the quantity of air or water vapor entering the package would be too limited to result in mechanical failure of the basket over potential storage intervals.

Corrosion Performance for Basket After Disposal. Following disposal, the basket will remain dry until the overpack and canister shell are penetrated. Once this happens, ground water could enter the package, and corrosion of basket materials could begin. If corrosion damage is extensive then mechanical failure (i.e., collapse) of the basket could occur, and increased reactivity.

Basket failure could occur through general corrosion if the metal walls of the cells holding fuel assemblies thin sufficiently to cause basket collapse. Localized corrosion in the form of pitting, if randomly located on the basket materials, might result in penetration of the cell walls, but would be unlikely to weaken the basket structure. However, localized corrosion (pitting, crevice, or stress corrosion cracking) in specific regions such as weight-bearing contact areas, or in weld zones, could weaken the structure. Basket materials should be selected with general corrosion rates that are too slow to allow structural collapse in 10,000 years. Further, basket materials should not be susceptible to localized corrosion that could result in failure within that time period, either because the materials are inherently not susceptible, or because they have been treated to reduce susceptibility (e.g., treatments to minimize weld residual stresses and sensitization due to weld heating).

2.3 Neutron absorber materials

Current neutron absorber materials are largely aluminum-based materials (Boral®, Metamic®) that corrode readily on immersion in water. Also, aluminum-based materials will act as sacrificial anodes relative to steels. Should canister breach occur during storage, some corrosion of aluminum-based neutron absorbers may occur due to water vapor and air entering the canister; however, this is unlikely to result in significant loss of the absorber, or in canister flooding that could cause criticality.

Aluminum-based materials exposed to water in a canister that is flooded after disposal will corrode rapidly, blistering and sloughing. Depending upon the types of fuel assemblies contained, the loss of neutron absorber from even a single cell could result in criticality. Aluminum-based neutron absorbers may not be appropriate for use in disposal systems, unless a strategy can be identified that does not rely on these absorbers, for how the canisters will remain subcritical when flooded (Hardin et al. 2014). Alternatively, such a strategy could be based on evaluations that breach of the disposal overpack and subsequent flooding are sufficiently unlikely (Hardin 2013).

Other materials, less susceptible to corrosion, should be considered if neutron absorbers are desired to function in the disposal environment. These include borated or gadolinium-containing stainless steels. While other elements can act as neutron absorbers, boron and gadolinium are effective and are easily incorporated into steels. Previous corrosion studies with 304B SS (Lister et al. 2007) using very dilute test solutions considered relevant to the Yucca Mountain Project, indicated that it performed well under those conditions, corroding at less than 0.05 $\mu m\ yr^{-1}$. However, repository conditions in a clay or granite repository could be considerably different than those tested. For a salt repository, analyses have shown that flooding with chloride brine would likely provide enough natural chlorine to ensure subcriticality (Hardin et al. 2014).

3. ENVIRONMENTS

3.1 Interim Storage Environment

Upon discharge from a reactor, fuel assemblies are stored in fuel pools for several years (typically 5 years or longer) until cool enough for dry storage. Transfer to dry storage takes place at the reactor sites, generally using thin-wall DPCs that can be handled in transfer casks, storage casks, and transportation casks. DPCs are welded stainless steel (304SS; Hanson et al. 2012) containers, intended as interim storage until a permanent disposal site is developed. In 2011, 10 CFR 72.42(a) was modified to allow for initial dry storage license periods of up to 40 years, and extensions of up to 40 years. However, the U.S. does not currently have a disposal pathway for SNF, and these containers may be required to perform their containment function for decades beyond their original design criteria. A few license renewals for existing containers have already been carried out, and at some point, all existing containers will have to be recertified.

Of primary concern with respect to the long term performance of the storage casks is localized corrosion. General corrosion does not occur under atmospheric exposure conditions, but various forms of localized attack such as crevice corrosion or SCC may occur if certain combinations of aggressive contaminants and humidity are present.

Most dry storage systems rely on natural convection to cool the canisters within the overpacks, and large volumes of outside air are drawn into the annulus. Dust and aerosols in the air are deposited on the steel canisters, and as they cool over time, salts in the dust can deliquesce to form brine on the canister surfaces. Localized attack can occur under deliquescent conditions. SCC of welded zones is of special concern, as it a well-documented mode of attack for austenitic stainless steels (including 304 and 316 SS) in marine environments (Kain 1990). Several experimental studies (e.g., Nakayama 2006; Tani et al. 2009, 2010; Mintz et al. 2012; Prosek et al. 2009, 2014; NRC 2014) have observed SCC under conditions nominally expected to occur on the surfaces of canisters stored near bodies of salt water.

Research on SCC of interim storage systems that are currently in use is being carried out at Sandia National Laboratories for the Used Fuel Disposition (UFD) Program. Other organizations, including the NRC and universities funded by the Department of Energy Nuclear Energy University Programs (NEUP), are performing similar evaluations. These other efforts are focused on existing in-service canisters, made from 304 or 316 SS, for which the welds were not mitigated to relieve residual stresses. For future casks, the constraints on material composition and stress mitigation are not applicable. Here, this study evaluates alternative materials, and materials processed to mitigate weld-related stresses and sensitization. These new materials will be less susceptible to atmospheric chloride-induced SCC.

3.2 Repository Disposal Environment

This study proposes testing to evaluate corrosion characteristics of candidate materials for the shells and internals of future SNF canister designs. As per 10 CFR 72.236(m), post-closure repository performance must be considered in designing storage canisters. Given that only generic (non-site specific) repository studies are currently underway, there are few constraints on possible disposal environments. Potential host rocks include salt (bedded or domal), shale or clay, and crystalline rock.

As noted previously, corrosion properties of the canister shell are not considered to be important to the containment performance of the waste package after disposal. We concentrate here on the basket and neutron absorber materials.

In the disposal environment after repository closure, the main functions of the basket and neutron absorber materials serve to reduce the risk of criticality. In salt formations, brines are saturated with halite and other salts, and have chloride concentrations greater than 5 molal. At chloride concentrations above approximately 2 molal, neutron absorption by natural chlorine is sufficient to ensure subcriticality (Hardin et al. 2014)., and the corrosion lifetimes of the basket and neutron absorber materials are not important. Accordingly, in the following discussion only argillaceous and granite-based repository environments are considered.

Environmental factors, including concentrations of chemical species, temperature, and pH affect iron and steel corrosion rates. General corrosion is generally faster under oxic conditions, as oxygen provides an additional electron acceptor. Oxic conditions also generally favor localized corrosion processes, which are associated with localized gradients in redox potential. Chloride and fluoride destabilize passive films in stainless steels, resulting in pitting if concentrations are sufficiently high, and increase general corrosion rates as well (Kursten et al. 2004; Smart et al. 2004). Other anions (sulfate, hydroxide, nitrate, carbonate) generally inhibit corrosion, via either competitive sorption or the formation of more protective films. Temperature generally increases corrosion rate, because it is an activation-controlled reaction. Temperature can also change the corrosion products, affecting their ability to form a protective layer. At elevated pH (>10) iron materials form a passive film and corrode very slowly. However, as the pH drops the corrosion rate increases until passivity is lost; the actual value at which this occurs depends on other environmental parameters (e.g., chloride concentration, temperature, redox potential). Decreasing pH also moves the pitting potential in the active direction, eventually resulting in pitting. However, once initiated, pit propagation may be independent of bulk solution pH because corrosion in the pit generates its own environment.

3.2.1 Repository depths and pressures

It is reasonable to restrict conditions to those for a mined repository, or to maximum depths of 1 km. This corresponds to a maximum hydrostatic pressure of 10 MPa, and a maximum lithostatic pressure (which may control hydrogen pressure) on the order of 22 to 26 MPa. In fractured, crystalline host rock the hydrostatic pressure will generally be that of an equivalent water column at the repository depth, while in a low-permeability shale the pore pressure will generally lie between the lithostatic and hydrostatic pressures.

3.2.2 Potential water/brine compositions

The range of potential pore water compositions in crystalline and argillaceous environments is large (Hardin et al. 2014). Table 1 illustrates the range of water compositions present in each environment. In both argillaceous rocks and crystalline basement rocks, water compositions can vary from dilute solutions to highly concentrated brines. This is in part a function of depth—the data in Table 1 are not limited to shallower depths. But even within a kilometer of the surface, large variations in composition are observed within the two host-rock types.

Figure 1 shows chloride concentrations as a function of depth in crystalline basements around the world. Although there is a general increase in salinity with depth at any given location, chloride concentrations within 1 km of the surface can still be as high as several molal (several tens of thousands of mg/L in Figure 1). Formation waters in granites are dominantly fracture waters, and owe their salinity and composition to many different processes, including downward percolation from overlying formations, upwelling hydrothermal waters, and long-term water-rock reactions (Frape et al. 2003). Crystalline rock pore waters are commonly anoxic below depths of a few hundred meters, and can contain variable concentrations of sulfide (pyrite is a common fracture mineral in crystalline rocks, for example, see Andersson et al. 2007).

Table 1. Range of geochemical conditions in three main geologic repository types (concentration values in mg L^{-1}).

Parameter	pH	Na^+	K^+	Ca^{2+}	Mg^{2+}	Cl^-	SO_4^{2-}	HCO_3^-
Crystalline Rock								
High	–	63,900	17,678	108,747	15,306	212,280	3,206	525
Low	–	10	0	9	0	2	1	2
Mean	–	7,490	542	15,283	1,106	40,926	317	85
Median	–	2,935	19	3415	25	10,186	114	54
Argillaceous Rock								
High	12	126,957	1,575	37,300	22,632	204,000	15,000	8,150
Low	1.04	3	3	1	1	6	1	4.56
Mean	7.39	19,099	135	3,088	708	35,830	1,270	964
Median	7.3	12,143	48	1,140	290	21,588	682	448
# data pts	7 10	772	167	787	776	794	721	762

Modified from Table 8-2, Hardin et al. (2014); see that document for a description of data sources.

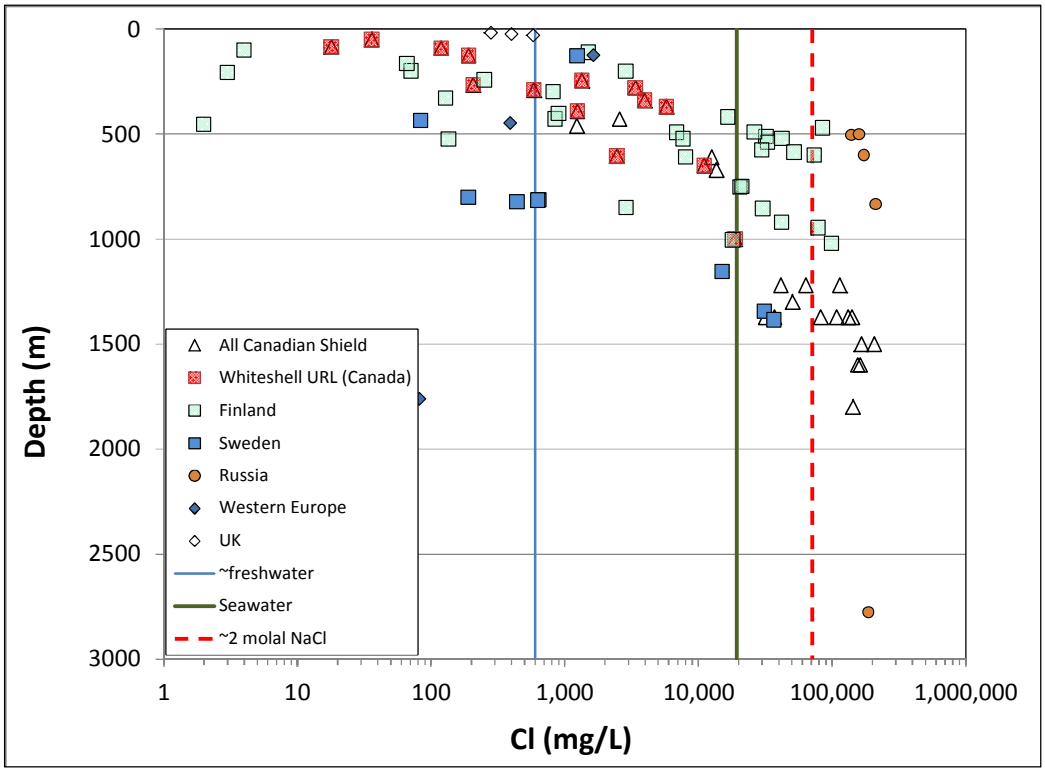

Source: Frape et al. (2003). Reference lines are the chloride concentration limits for fresh water and average seawater, and the chloride concentration for 2 molal NaCl. Reference lines are the upper limits of chloride concentration for fresh water and average seawater, and the chloride concentration of 2 molal NaCl brine.

Figure 1. Chloride concentration vs. depth for various crystalline terranes (from Hardin et al. 2014).

Data for shales in sedimentary basins show similar trends (Figure 2). In any given sedimentary basin, salinity increases with depth, and while formation pore waters are very dilute in some formations, in others, very saline brines may exist close to the surface. As with crystalline rock pore waters, several factors can contribute to salinity in shales, including infiltration of highly saline water from other units in the sedimentary basin and long-term water rock interactions. Pore waters are anoxic; shales commonly contain percent levels of organic material, and pyrite is common as a minor phase.

The data in Table 1 and in Figures 1 and 2 are presented to illustrate the potential range of ground water composition in a repository. More complete discussion of pore water compositions in potential repository host rocks is provided elsewhere (Hardin et al. 2014). For each potential host rock type, it is clear that corrosion performance should be evaluated for a suite of different water compositions.

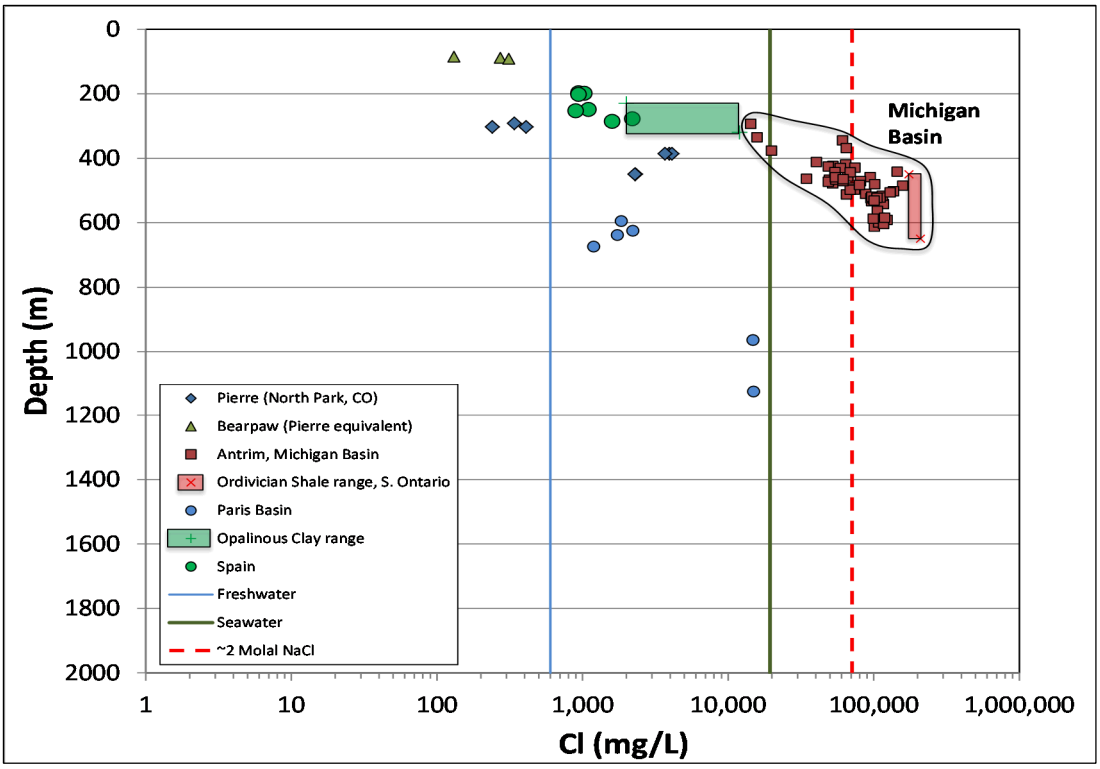

Source: Hardin et al. 2014, Figure 5.3. See that document for original data sources.

Reference lines are the upper limits of chloride concentration for fresh water and average seawater, and the chloride concentration of 2 molal NaCl brine.

Figure 2. Depth vs. chloride concentrations vs. depth for selected shale formations in North America and Europe (from Hardin et al. 2014).

3.2.3 Redox conditions

For testing purposes it can be reasonably assumed that eventual penetration of the overpack and canister wall will occur long after any oxygen trapped in the near-field or clay barrier has been consumed by corrosion of the metal overpack or by reactions with organics or sulfides in the host rock.

Alpha radiolysis of water is unlikely to result in significant oxic corrosion of the canister components. Both oxidizing radicals and reducing species (such as H_2) are formed by alpha radiolysis of water in the immediate vicinity of SNF pellets. They tend to catalytically recombine on the surface of the fuel pellet (Jerden et al., 2013). Conceivably, the oxidizing radicals could react more quickly with iron metal or with ferrous iron in solution, prior to recombining. However, this possibility can be simplified by considering two cases:

- The oxidizing and reducing products of radiolysis recombine on the fuel surface. Metal corrosion will therefore be anoxic, occurring through breakdown of water, and hydrogen buildup will occur, which would further drive recombination of the oxidizing and reducing species at the fuel surface.
- Oxidizing radicals react with metal or ferrous iron in solution. They are no longer available to react with hydrogen and recombine on the fuel surface, so, again, hydrogen builds up, until recombination at the fuel surface is again favored.

Accordingly, testing will be initiated using deoxygenated water, and oxygen or oxidizing radicals will not be added. Over time, H_2 may build up in the test systems (as it could in the disposal environment). However, it will not significantly inhibit corrosion unless the H_2 partial pressure is very high; such inhibition could require H_2 pressure greater than the hydrostatic or even lithostatic pressure at typical repository depths. Hence, running tests at elevated H_2 pressure is not expected to produce repository-relevant data. We note however that elevated H_2 concentrations can lead to embrittlement of certain metals and mechanical failure, so some tests will be run at pressure to evaluate the effects of hydrogen build-up.

3.2.4 Temperature range

The timing of pore water entry is unknown, and temperatures may still be somewhat elevated relative to ambient temperatures due to decay heat, although high temperatures are unlikely. To evaluate the temperature dependence of corrosion reactions, tests are proposed over a range of temperatures from 25 to 60ºC. Interpretation of corrosion mechanisms may also be informed by elevated temperature test results.

3.2.5 General experimental design

Once the waste package/overpack is breached by localized corrosion, high external pressures will force water through the breach and into the waste package. It is assumed that intrusion of clay backfill material or host rock will be minimal. Then, the waste package can be considered a batch system, consisting of the ground water, the waste package internals (basket and neutron absorber), and the waste assemblies.

Potentially important aqueous species can then be divided into two groups:

- Species that are present in excess. These species are unlikely to be consumed by corrosion reactions as rapidly as they are replaced by diffusion. This includes water, which will be the primary oxidant for the metals under anoxic conditions, and chloride, which will be present in high concentrations. The concentrations of these species can be held constant.
- Species such as hydrogen sulfide that are present in low concentrations and will rapidly be consumed by corrosion reactions. The rate of reaction will be equal to the rate of diffusion or advection into the package. The pH will also vary, but will be controlled by reactions within the package.

Corrosion tests to assess material performance under repository conditions will be carried out in closed, pressurized batch systems, with excess amounts of water/brine. Initially, simplified systems of water and sodium chloride at varying concentrations will be used, to assess the effect of chloride concentration. Later, systems containing representative pore waters will be used to assess the formation and composition of the passive layer, and the corrosion rate. Initial pH values will be near-neutral, but will be allowed to vary as the corrosion reaction proceeds. Hydrogen sulfide-containing systems will be used to assess the effect of sulfide on corrosion rates and corrosion products, but no attempt will be made to control or buffer the sulfide concentration, as it is anticipated that under repository conditions, such reactions will be transport-limited.

4. CANDIDATE MATERIALS AND MATERIAL TREATMENTS

Because an overpack can be assumed for disposal, needed corrosion performance for the canister shell is limited to that relevant to interim storage. The only corrosion mechanism that is likely to cause canister failure in this context is stress corrosion cracking. To reduce this risk, expensive or exotic materials are not required. Instead, other steels less susceptible to SCC will be considered, and also weld mitigations that could reduce the susceptibility of 304 or 316 SS to SCC.

For basket materials, corrosion properties of 304 and 316 SS under potential repository conditions are the subject of another test plan, to assess performance of components of existing DPCs under argillaceous or granitic repository host rock conditions (Ilgen et al. 2014). Here, other metals that are more corrosion-resistant are also considered—these are mostly different types of stainless steel, but also include Hastelloys. Also, weld-mitigated 304 and 316 SS will be evaluated, as these are not being used in current DPCs, and are not identified in the DPC test plan. The performance of neutron absorber materials, including borated and gadolinium doped stainless steel, is also addressed in the proposed testing.

This section provides a description of the general groups of stainless steels and their properties. The term *stainless steel* is used to describe a group of iron-chromium alloys, many containing nickel, that are more resistant to corrosion and rusting than non-chromium containing steel. Stainless steels are designed to have very good resistance to corrosion in aqueous environments, acidic solutions, and at high temperatures (Hosford 2012; Lai et al. 2012; Outokumpu 2013). A steel must contain at least 11 wt% chromium to exhibit good resistance properties in benign environments and to be designated as stainless. When a steel is resistant to corrosion it is labeled as passive, and for a stainless steel to exhibit passivity in harsh environments either a larger

chromium content or additional alloying elements are necessary (Hosford 2012). There are five major types of stainless steels that are classified based on their microstructure at room temperature: ferric, austenitic, duplex, martensitic, and precipitation hardening. It should be noted that the last two types are sometimes grouped together.

Ferritic stainless steels. Ferritic stainless steels contain 11.5 to 30% chromium, minor amounts of silicon and manganese, and minimal carbon and nickel content (Hosford 2012; Outokumpu 2013). Pure Fe-Cr alloys have a body-centered cubic (BCC) structure, and are magnetic. Ferritic stainless steels are used for architectural and automotive trim.

Austenitic stainless steels. By mass percent, austenitic stainless steels are the most widely world-wide (Lai et al. 2012). They contain 17 to 25% chromium, 8 to 20% nickel, and a minimal amount of carbon (Hosford 2012). The presence of nickel, carbon, manganese, and nitrogen stabilizes the face-centered cubic (FCC) austenite phase over the ferrite phase. This steel grade has very good corrosion resistance, and is nonmagnetic (Outokumpu, 2012). The FCC crystal structure prevents embrittlement at low temperatures, and these steels are often used for cryogenic applications. Austenitic steels are categorized in the AISE-SAE system with 2xx and 3xx designations. Austenitic steels can be further subdivided depending on the main alloying elements into Cr-Ni, Cr-Mn, Cr-Ni-Mo grades, and high performance austenitics, also referred to as super-austenitics (Hosford 2012).

Heating to 600 - 650ºC, or slowly cooling through this temperature range, may reduce the corrosion resistance of austenitic and ferritic steel grades containing more than 0.03% carbon. When these conditions are met, chromium and carbon will diffuse to the grain boundaries and form chromium-rich carbides ($(Fe,Cr)_{23}C_6$) at the grain boundaries, reducing the chromium content in nearby regions. Once the local chromium content decreases to below ~12%, intergranular corrosion can occur at grain boundaries (Hosford 2012). This process is known as sensitization, and it can occur in the heat affected zones (HAZ) in welded austenitic stainless steels with sufficient carbon content. The weld itself is not sensitized, as it crystallizes from molten metal, and is annealed. Sensitization, in combination with weld residual stresses, reduces the corrosion resistance of austenitic stainless steels, and, in sufficiently corrosive environments, can support SCC.

Duplex stainless steels. Duplex stainless steels have a mixed austenite-ferrite microstructure in an ideal ratio of 50/50. Duplex stainless steels are both stronger and have better resistance to pitting corrosion, crevice corrosion, and stress corrosion cracking than austenitic steels (Hosford 2012). This steel grade has a high chromium content of 19 to 28% and a maximum value of 5% molybdenum (Hosford 2012); they have a lower nickel content (1.4 to 7%) than austenitic stainless steels (Outokumpu 2013). Addition of small amounts of molybdenum, tungsten, and copper improves corrosion performance even further, and makes them super-duplex. These steels are magnetic.

Martensitic stainless steels. Martensitic stainless steels contain 12 to 17% chromium and 0.1 to 1.0% carbon (Hosford 2012). The higher carbon content than other stainless steels improves the strength and hardenability of this grade (Outokumpu 2013). They are primarily used for razor blades, knives, and cutlery (Outokumpu 2013). Martensitic steels have high strength and high

wear resistance (Outokumpu 2013). They are categorized in the AISE-SAE system as 4xx and are characterized by the martensite (body-centered tetragonal, or BCT) crystal structure.

Precipitation-hardening stainless steels. Precipitation-hardening stainless steels are formed from an austenitic or martensitic base plus copper, titanium, aluminum, molybdenum, and niobium (Hosford 2012). They contain little or no copper. They are categorized in the AISE-SAE system as 6xx and are characterized by the precipitates that form in the microstructure during processing, impeding the movement of dislocations and resulting in an increase in the hardness of the steel.

Many of these grades offer greater hardness or lower cost than 300 series austenitic stainless steels, but do not compare in terms of ductility or corrosion resistance. However, super-austenitic, duplex, and super-duplex stainless steels offer comparable mechanical properties and better corrosion performance than 300-series steels at a similar or somewhat higher cost. The next step up from these in terms of corrosion resistance are the nickel alloys C-22 and C-276. Moreover, these metals similar enough to standard 300-series steels that no galvanic reactions will occur.

4.1 Choice of candidate materials for testing

For canister shell materials, the effects of weld mitigations (laser or shot peening; post-weld annealing) will be assessed on 304 and 316 SS. Ideally, this would be sufficient for a standardized canister, as it would potentially economically mitigate the only corrosion concern for the canister shell, which is SCC during interim storage. Super-austenitic, duplex, and super-duplex steels will also be considered.

For basket materials, the same suite of steels will be evaluated, but the nickel alloys will also be considered. The desired corrosion performance of the basket materials is potentially more difficult to meet, as a far longer time interval for corrosion must be considered.

For neutron absorbers, standard borated stainless steel and Gd-containing 316 SS will be considered. Borated stainless steel is in use on some current DPCs, and Gd-containing stainless was evaluated for use on the Yucca Mountain Project in the early 2000s, and found to have good corrosion properties (Mizia et al. 2001).

For each of these, three treatments will be applied. Experiments will be done with polished and pickled base metal, with a weld/HAZ sample, and with weld samples that have been mitigated by peening burnishing, or annealing after welding. Coupon tests will be done to measure general corrosion rates and pitting corrosion, and U-bend samples to assess the potential for stress corrosion cracking. Experimental methods are described in the following section.

5. CORROSION TESTING METHOD

5.1 General corrosion

General corrosion typically manifests as a uniform recession of the metal surface with time. Dissolution rates depend on environmental parameters including the solution chemistry, oxygen availability, temperature, and mass transport limitations. The environment of concern is that

which forms at the metal surface. For materials for which the dissolution rate is low and/or mass transport occurs rapidly, the environment at the surface can be nominally identical to that of the bulk solution far from the metal surface. Conversely, for materials for which the dissolution rate is high, or for which mass transport is limited, metal ions from the corrosion process (and any resulting corrosion-product precipitates) can have a significant impact on the local chemistry. Two different examples are: 1) hydrolysis by metal ions can dramatically reduce pH, potentially accelerating corrosion; and 2) saturation of the local solution with metal ions can result in precipitates that significantly limit mass transfer to the metal surface, inhibiting corrosion.

To evaluate the long-term general corrosion rate, it is important that the environment at the metal surface be characterized so that the behaviors described above are recognized. There will likely be an initial transient period during which the corrosion rate starts high, then decays to a steady value. Alternatively, if the environment becomes more aggressive as metal ions build up, the corrosion rate may start low then increase to a steady value. Assessing the long term general corrosion rate can be done using a variety of techniques, broadly characterized as active electrochemical techniques, or un-instrumented immersion experiments. Both are described below.

5.1.1 Un-instrumented (weight-loss)

Immersion testing is the simplest way to measure the general corrosion rate. A variety of industry-standard procedures exist, including the combination of ASTM G1 and ASTM G31. The sample is placed in the test environment for a fixed period of time and observed on completion. The specimen is weighed prior to being placed into solution. At completion the sample is de-scaled (removing all corrosion product while minimizing any removal of the base metal) and the weighed again. The weight change is converted to a corrosion rate either in terms of mass loss per unit area per time (where the area is the total exposed surface area of the specimen). This can be converted to a corrosion rate in terms of depth vs. time by using the density of the metal. The resolution of this measurement is the minimum measureable weight change per unit area of the sample per time. For passive metals, such as stainless steels, the general corrosion rate is very small, equivalent to the passive current density. For such materials weight loss can still be used provided that the exposure time period is long enough, de-scaling is controlled, and the weight measurement is sufficiently sensitive. High precision balances are needed, coupled with a well-defined measurement procedure such as the NIST single substitution methods (NIST SOP no. 7).

5.1.2 Instrumented (electrochemical)

Electrochemical testing can also be used to extract the general corrosion rate. This is accomplished by measuring the polarization resistance of the surface, then using the Stern-Geary equation. The procedure is described in ASTM G59, then the conversion of the polarization resistance to a corrosion rate in ASTM G102. In essence, the polarization resistance is determined by scanning the applied voltage across the open circuit potential. The magnitude of the applied potential must be sufficiently small that the voltage vs. current curve is linear (values of 5 to 20 mV are typical). The polarization resistance is then calculated as the slope of the voltage vs. current curve.

$$\text{Polarization Resistance} = R_P = \frac{\partial E}{\partial I} = \frac{\Delta E}{\Delta I} \text{ where } \Delta E \text{ is small, and taken about } E_{ocp} \quad (1)$$

This polarization resistance is then converted to a corrosion current density, i_{corr}, via the expression derived by Stern and Geary from the Nernst equation:

$$i_{corr} = \frac{B}{R_P} \text{ where } B = \frac{b_a * b_c}{2.303*(b_a + b_c)} \quad (2)$$

Where B is the Stern-Geary constant, b_a the anodic Tafel slope, and b_c the cathodic Tafel slope. A second set of experiments is used to acquire the Tafel slopes. Calculation of the Tafel slope requires that an anodic polarization experiment be performed on the material of interest to extract the anodic slope, and a cathodic polarization experiment for the cathodic slope. The applied potential is slowly scanned from near the open circuit potential in the desired direction. In most cases, a plot of the applied potential vs. the log of the current density will be linear, and the slope of this linear region is the Tafel slope.

$$b = \frac{\partial E}{\partial(\log(i))} \quad (3)$$

Once the anodic and cathodic Tafel slopes have been determined, the polarization resistance can be converted to the corrosion current density. Conversion of this current density to a corrosion rate (in mass or depth per unit time) requires some additional estimates. For a pure metal, the oxidation reaction can be described as:

$$M \rightarrow M^{n+} + ne^- \quad (4)$$

Conversion of the current density for that reaction to the corrosion rate requires that the mass of metal that will be oxidized by the passage of 1 Faraday (96489 Coulombs) of electrical charge. This is called the equivalent weight, and is equal to the molecular weight of the metal divided by the number of electrons passed in the oxidation reaction. For example, considering iron, if it was being oxidized to the +2 valence state, then the equivalent weight would be (55.845 g/mol)/2, or 27.9 g/equivalent. If, however, the iron were being oxidized directly to the +3 valence state, the equivalent weight would be 18.6 g/equivalent. Clearly, knowledge of the specific reactions at the surface is critical for this calculation. In the case of an alloy such as Hastelloy C276, determination of the equivalent weight is more complicated as there are multiple constituents that are part of the dissolution process. The nature of the individual reactions (in terms of the number of electrons passed for each constituent) will vary with the environment to which it is exposed. E-pH diagrams (i.e., Pourbaix diagrams; Pourbaix 1974) can be used to determine the likely valence states of each constituent, and values for common alloys are tabulated in ASTM G102.

Both electrochemical and immersion (weight loss) techniques can accurately measure the general corrosion rate, but both have limitations, particularly when corrosion resistant materials such as stainless steels or nickel-chromium alloys are explored under conditions where their corrosion rates are very low (i.e., the materials are passive). For the electrochemical tests, there are a

number of kinetic parameters that must be defined in order to extract the corrosion rate from the polarization resistance. Further, as the conditions that exist at the metal surface may vary with time during a test, the reactions (in terms of the resulting valence state from the oxidation reactions) may change. As a result, the equivalent weight for the alloy being evaluated may change, further complicating determination of the corrosion rate.

5.2 Localized corrosion

Passive materials such as stainless steels and nickel-chromium alloys typically exhibit a low general corrosion rate (defined by the passive current density). However, in the presence of aggressive ions such as chloride, thiosulfate, etc., they are prone to localized corrosion. Localized corrosion results from breakdown of the passive film, often at a microstructural heterogeneity such as a grain boundary or secondary phase precipitate, followed by focused dissolution of the underlying metal. This type of corrosion is generally manifested as pitting or crevice corrosion. The pitting process is illustrated in Figure 3. The life cycle of a pit can be broken down into a series of stages as shown. First, there is an event through which the oxide is locally broken down. This breakdown can be the result of a number of factors, singly or in combination, including accumulation of depassivating species (e.g., chloride) at the surface, dissolution of a secondary phase particle (e.g., a MnS inclusion) at the surface, or accelerated local attack due to some other microstructural heterogeneity such as a grain boundary. Once initiated, the pit begins to grow via oxidation of the metal. Once nucleated, the pit grows into the metal. While a hemispherical geometry is shown in the figure, in practice the actual geometry can be much more tortuous with higher aspect ratio. Active propagation requires that the solution chemical conditions within the pit are maintained. Solution conditions are formed and maintained by oxidation of metal ions, which in turn hydrolyze and reduce the pH. To maintain charge neutrality, aggressive anions such as chloride are drawn into the pit. Cathodic (reduction) reactions that support active dissolution within the pit, occur outside the pit on the metal surface. With time, pits often repassivate or growth may “stifle” when the critical chemistry can no longer be maintained. This can be the result of many different factors including a loss of the mass transport limitation imposed by the occluded pit geometry (e.g., the pit cover may collapse) or the inability of the external cathode to supply sufficient current to support metal oxidation within the pit due to IR (i.e., ohmic) potential drop or depletion of reactants. Mass transport of aggressive species such as chloride may also become limiting if the bulk environment is dilute, or the chloride source (e.g., a salt film on the metal surface) is depleted.

Crevice corrosion is similar to pitting in terms of the reactions, externally located cathode, etc. However, in the case of crevice corrosion an occluded geometry (i.e., the crevice) provides the driving force for initiation. The crevice corrosion process is illustrated schematically in Figure 4. As mentioned above, an occluded geometry is required. Initially, passive dissolution and oxygen reduction (or some other cathodic reaction) occurs on the metal surface both within and outside of the occluded region. Mass transport is limited both into and out of the crevice, and causes a gradual increase in the metal ion content and a decrease in the cathodic reactant (e.g., dissolved oxygen) within the crevice. This has several effects, the first of which is separation of the anodic region (metal oxidation inside the crevice) and the cathodic reaction (reduction of dissolved oxygen, etc. outside the crevice). The metal ions hydrolyze, decreasing the pH inside the crevice. Aggressive anions such as chloride are transported into the crevice to maintain charge neutrality,

further increasing the aggressiveness of the environment. Eventually, the solution is sufficiently aggressive to result in depassivation of the metal within the crevice, and the initiation of crevice corrosion. As with pitting, the crevice will remain active as long as the critical crevice chemistry is maintained. If the occluded geometry is lost (which can be the result of metal dissolution increasing the crevice gap), the mass transport limitation is lost and the crevice will repassivate. Similarly, if the supply of anions moving into the crevice is depleted or the capacity of the external cathode is exceeded, repassivation will occur.

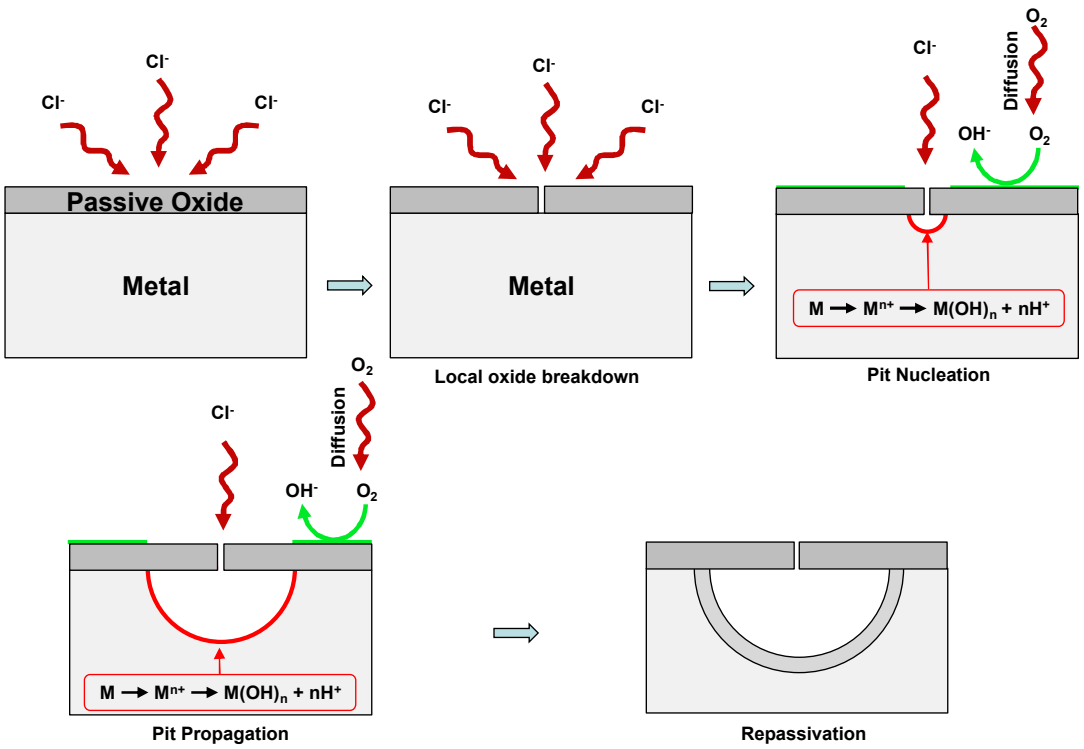

Figure3. Schematic representation of the nucleation, growth, and repassivation process for pitting corrosion.

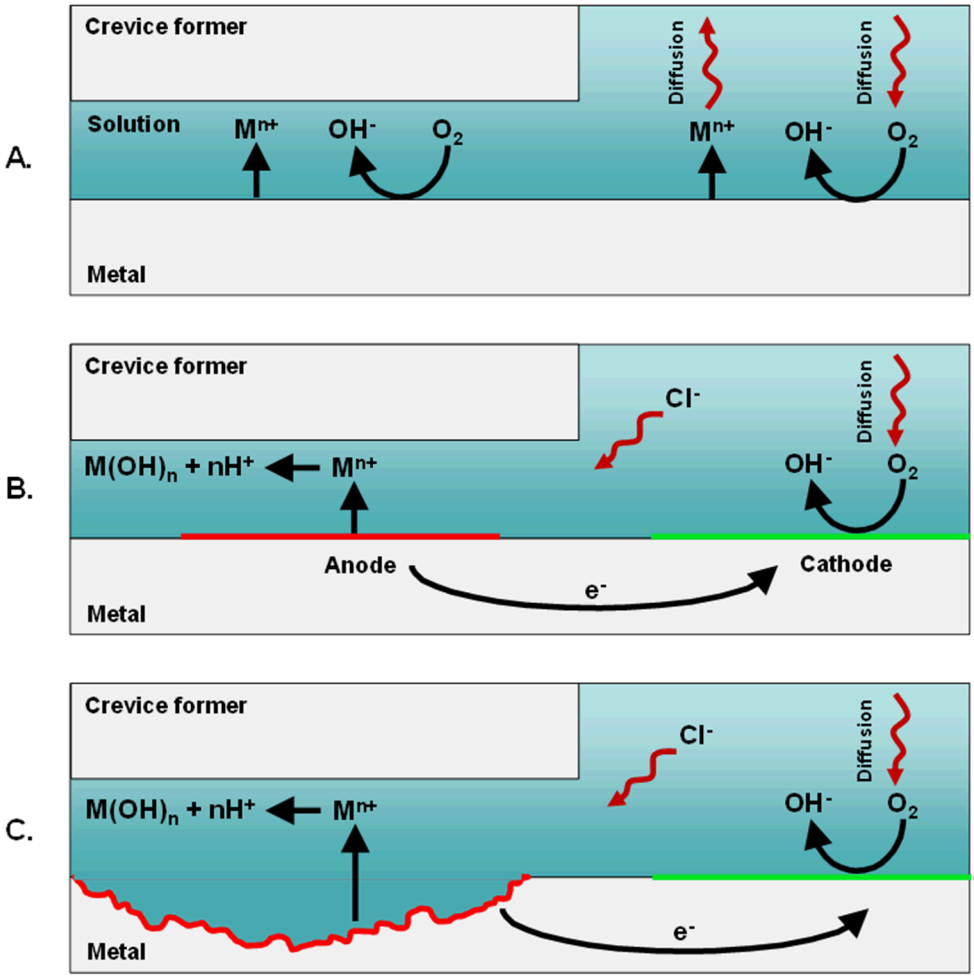

Figure 4. Schematic representation of the crevice corrosion initiation and propagation processes, indicating the type and location of pertinent reactions. While oxygen reduction is indicated as the primary cathodic reaction, other reactions could be viable.

Crevice corrosion is typically more readily initiated than pitting, on susceptible materials. When performing an experiment to evaluate and measure pitting corrosion, it is important that no crevices be present. The primary source of unintended crevices is the fixturing used to secure the sample, including gaskets or coatings used to define the region of the metal surface being studied. On completion of a test of pitting corrosion, visual inspection must be performed to verify that crevice corrosion did not occur.

When performing crevice corrosion experiments, an artificial crevice of known geometry is typically formed on the metal surface. This can be done by securing a multiple crevice-former assembly (MCA) or other similar construction onto the surface (Figure 5). The propensity for crevice corrosion to initiate is a strong function of the crevice geometry (e.g., by setting the tightness and thus the degree of mass transport limitation), the fixturing selected should represent a worst case view of what is anticipated to occur in practice. If the geometry is too tight, crevice

corrosion susceptibility may be indicated when it is not viable in the material application. Similarly, if the crevice geometry is too open, crevice corrosion may not initiate when a tighter geometry may exist in the application.

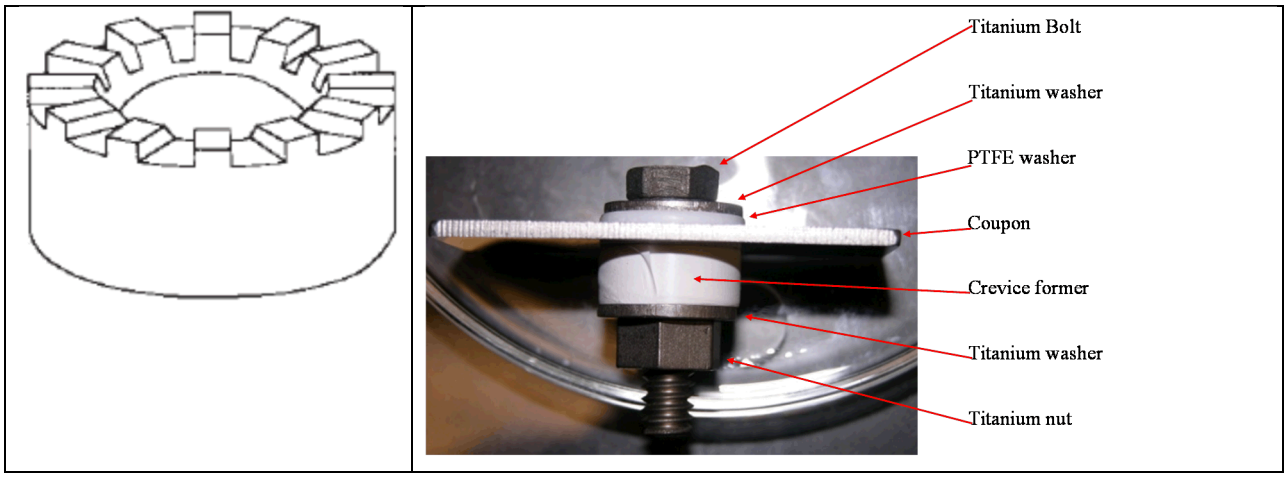

Figure 5. Multiple crevice former assembly (MCA) illustrated on the left, and a sample instrumented with an MCA on the right. Care must be taken to prevent electrical connection of the hardware used to create the crevice (i.e., the titanium fittings shown above) with the sample being evaluated.

5.2.1 Un-instrumented exposures (not driven)

As with general corrosion testing, immersion testing involves simply placing the samples of concern into the desired environment for a predetermined time period, then removing and inspecting the samples for damage. In the case of pitting corrosion, samples are prepared and placed into solution such that no unintended crevices are formed. In the case of crevice corrosion, samples are prepared with one or more artificial crevices on the metal surface. The surface finish and cleanliness of the coupons prior to initiation of experiments will impact the susceptibility of the material to either degradation mode, and should be consistent from test to test. Once prepared, coupons are introduced into the desired environment for a predetermined time period. Upon completion of the time interval, the samples are removed and assessed for the presence of localized corrosion. A general procedure for examination of localized corrosion is presented in ASTM G46.

The primary limitation of immersion tests is that each coupon can be used for a single measurement – removal from solution is effectively destructive from the viewpoint of the experiment. Thus, the selection of appropriately long time periods is critical. In other words, once a test is completed (i.e., the sample removed from solution), if no corrosion is observed the coupon cannot simply be reintroduced to the solution to allow the experiment to continue. Doing so would be effectively restart the experiment.

5.2.2 Electrochemical approach (driven experiments)

Electrochemical methods for determining the potential for pitting or crevice corrosion involve the identification of a series of critical potentials, illustrated schematically in Figure 6. An anodic polarization curve is performed (the arrows in the figure indicate the direction in which the applied voltage is scanned), the general procedure for which is described in ASTM G5. As the potential becomes more positive, the driving force for oxidation to occur on the surface increases. At this point, the dissolution rate is low, and the slope of the polarization curve is large. The current density in this regime is the passive current density. Passive materials are often referred to as being highly polarizable due to this behavior – in other words, large shifts in the applied voltage result in vanishingly small changes in the oxidation rate at the metal surface. When the applied potential becomes sufficiently large, local breakdown of the passive film results, and pitting initiates. On the polarization curve, this is manifested as a rapid increase in the measured current density as the applied voltage becomes more positive. At that point, there are one or more stable pits propagating on the metal surface. The direction of the polarization scan is then reversed, and the scan begins moving to less positive potentials. Initially, the current density will remain large, as the pits remain stable. When the potential has reduced to a sufficiently low level, the current density will decrease to below the previously measured passive current density. The point at which the polarization curve crosses itself is referred to as the repassivation potential (indicating that pitting is no longer actively propagating, and the sample has returned to a state of passive dissolution).

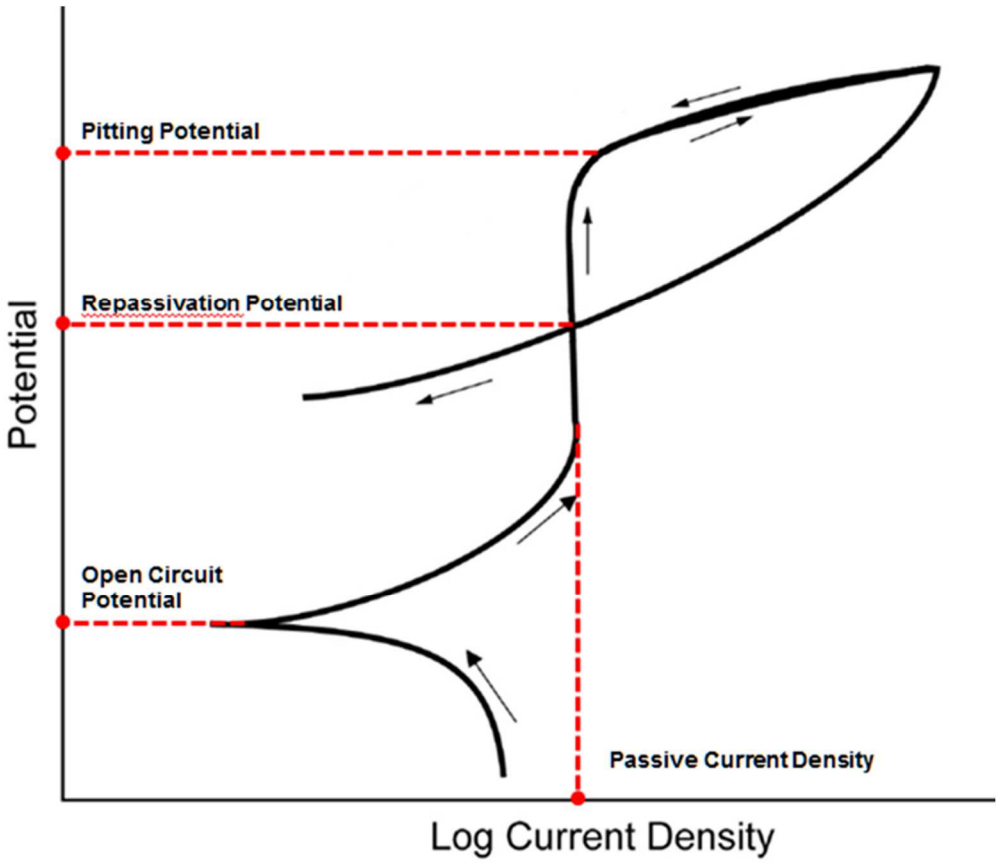

Figure 6. Schematic representation of an anodic polarization curve for a passive metal susceptible to localized corrosion. Indicated on the figure are the open circuit potential (i.e., the rest potential), the pitting potential, the repassivation potential, and the passive current density.

The pitting potential is not necessarily a well-defined value, and can vary from sample to sample. Factors which impact it include the surface finish of the metal coupon being evaluated, the underlying microstructure of the material (e.g., grain structure, secondary phase particles, etc.), and even the manner in which the experiment is run, such as the rate at which the potential is scanned in the experiment. For these reasons, the pitting potential is often not used as the critical potential at which stable pit growth is possible, and instead, the repassivation potential is used. The repassivation potential is thus taken as the critical potential below which pitting will not initiate.

Electrochemical crevice corrosion experiments are performed in essentially the same way, except that the sample is instrumented with a multiple crevice-former or similar device, and the potential at which a rapid increase in current is measured corresponds to the crevice corrosion initiation potential. The critical potential for crevice corrosion initiation is typically less positive than for pitting (i.e., it is “easier” to initiate localized corrosion when you have an occluded geometry such as a crevice, than nucleating a pit on a boldly exposed surface). If the system

under consideration is likely to have occluded geometries present, the approach generally taken is to determine the crevice corrosion behavior, rather than the pitting behavior, as it will represent a more conservative assessment of the risk of localized corrosion.

When polarization experiments are performed as described above, the surface should be inspected visually on completion to verify that localized corrosion did in fact occur. There are a number of other phenomena that will result in similar changes in measured current density with changes in potential. The two principal concerns are oxidation of water to form oxygen, and transpassive dissolution of the metal being evaluated. Both of these reactions occur at well-defined potentials, and will typically not exhibit the hysteresis illustrated in Figure 6. Transpassive dissolution occurs when the oxide on the metal surface is no longer thermodynamically stable, and results in very rapid dissolution across large portions of the sample surface, appearing similar to general corrosion on sample inspection. In materials where pitting or crevice corrosion can take place, the critical potentials for either phenomenon are less positive than the oxidation of water, or transpassive dissolution.

The critical potentials determined as described above can be used to assess the risk of localized corrosion for a particular set of environmental conditions. Typically, the long-term open-circuit potential of the metal of concern is monitored or modeled, and at the point where it becomes more positive than the repassivation potential, localized corrosion initiation may be conservatively assumed. This is quite conservative particularly for alloys that are passive under the environmental conditions being considered. As discussed previously, passive materials are typically highly polarizable – in other words, small changes in the current density can result in large shifts in the potential. In practice, if the open-circuit potential drifts to a potential more positive than the repassivation potential, in order for localized corrosion to propagate, the surface outside the localized corrosion site must supply sufficient cathodic current to support the oxidation occurring at the active surface (i.e., inside the pit or crevice). Since the surface is highly polarizable, if the cathodic reaction rate is increased on the surface, the potential will rapidly shift in the cathodic direction (i.e., become less positive than the critical potential for localized corrosion initiation). As a result, conditions will no longer be favorable for localized corrosion propagation, and the site will repassivate. Thus, while the repassivation potential can be used as the lower bound to where localized corrosion can initiate, in practical terms, the potential must be significantly more positive than the repassivation potential in order for localized corrosion to occur. The reason localized corrosion can occur at potentials more positive than the repassivation potential for driven experiments (from which the critical potentials were derived) is that the cathode is removed from the metal surface under driven experiments, and the rate of reaction at the cathode does not have the same stifling effect on the potential of the metal surface as it does in an un-driven experiment.

5.3 Environmentally assisted cracking

In addition to corrosion at the metal surface, the components of the container or container internals may be susceptible to environmentally assisted cracking. There are two forms that are of concern here – stress corrosion cracking and hydrogen embrittlement. Stress corrosion cracking is, in many ways, analogous to localized corrosion in that there is an active corrosion front (i.e., the crack tip) and a cathodic area supporting that dissolution process, typically located

at the metal surface (i.e., outside of the crack). In order for stress corrosion cracking to occur, three things are needed. First, the material must be susceptible to stress corrosion cracking. Second, there must be a sufficiently aggressive environment, and finally, there must be a sufficiently large stress to support propagation of a crack. For an experimental study of whether or not there is a risk of SCC in a particular application, the first two may be suspected (but not known) based upon a literature review or similar study, but the third (the presence of stress) should be known. In other words, the goal of the testing is to determine if the material under considering will crack under the exposure conditions of interest, but there is no need to pursue such testing if there are no stresses (either applied or residual) present.

There are two aspects to the stress corrosion cracking process that must be understood – the first is the nucleation behavior and the second is the propagation behavior. Nucleation is a particularly difficult aspect to study in a definitive manner, as there may be very long induction periods before cracking initiates. These induction periods can be associated with changes in the surface chemistry of the material or the initiation and propagation of other degradation modes, such as pitting, which result in a stress riser and serve as an initiation site. A variety of techniques have been employed to assess the risk of crack initiation, these include U-Bend specimens (ASTM G30), C-ring specimens (ASTM G38) and bent beam specimens (ASTM G39). Such specimens provide a pre-stressed specimen which can be exposed to a variety of aggressive environments. In the case of U-bend specimens, the sample is subjected to a combination of elastic and plastic (i.e., permanent) deformation, whereas for the bent beam specimens (including 2, 3, and 4 point bend tests), the loading is typically elastic in nature. Samples are loaded, then exposed to the desired aggressive environment. Periodic inspections are then performed to determine if/when crack initiation takes place. Unfortunately, due to the tortuous nature of stress corrosion cracks, the poorly defined crack geometry, and stress distribution that changes with crack extension, extraction of crack growth rate data from U-bend, bent beam, or C-ring specimens is difficult.

In order to effectively measure crack growth rates, specimens which have a known stress state, and which promote a well-defined (and understood) crack geometry are needed. This is typically done using specimens and test techniques that mimic what is done when assessing the plane strain fracture toughness of materials. Procedures for this are generally defined in ASTM E399, E1304, and E1820. Crack growth rates are monitored via techniques such as direct current-potential drop (DCPD) where a large current is passed through the sample while being evaluated. The specimen acts as a resistor, with the voltage drop across the specimen increasing as the crack extends into the material. Experiments may be performed using traditional compact tension test specimens, as illustrated in ASTM E1820, however, use of such systems is complicated due to the need to maintain the environment at the crack mouth. A variety of methods have been explored to accomplish this, including adding an electrochemical cell which allows solution to be passed across the crack mouth. Another method to perform SCC crack growth rate testing is through the use of double-cantilever beam specimens, as discussed in ASTM G168. The specimens are typically loaded through the use of bolts, and can be instrumented with DCPD or similar sensors to measure crack growth rate as a function of time, though often simple measurements of the crack length along the sample side are used to gauge the crack growth rate. These specimens have the advantage of being readily introduced into an aggressive solution without placing high-dollar mechanical test equipment at risk.

In some repository scenarios, cathodically generated hydrogen (accompanying metal oxidation) is anticipated to build in pressure due to the low permeability of the surrounding overpack, buffer/backfill material, and/or host rock. As such, there is a concern that hydrogen embrittlement of the materials may occur. There are a variety of mechanisms through which hydrogen can adversely impact the mechanical properties of a metal, and a thorough discussion is beyond the scope of this document. In general, the end result of hydrogen uptake is a reduction in ductility and ultimate strength, and an overall more brittle nature of the cracking process. For austenitic stainless steels and nickel based alloys, the susceptibility to hydrogen embrittlement increases with increasing yield strength (i.e., annealed materials are far less susceptible than work or precipitation hardened materials). Numerous factors impact the susceptibility including the aforementioned strength, along with the composition, microstructure, and fugacity of hydrogen present.

6. CONCLUSIONS

This document identifies materials and material mitigation processes that might be used in the design of a standardized canister for storage, transportation, and disposal of SNF. Potential corrosion modes and processes are addressed, which should be taken into account in canister design. The major potential corrosion risk during storage is stress corrosion cracking of the weld regions on 304 or 316 SS canister shells due to deliquescence of chloride salts on the surface. Here, two approaches are proposed for alleviating this. First, the existing canister materials (304 and 316 SS) could be used but the welds mitigated to relieve residual stresses and/or sensitization. Alternatively, shells could be fabricated from more corrosion-resistant materials such as super-austenitic or duplex stainless steels. Corrosion testing is needed to verify that these alternatives would successfully reduce the risk of stress corrosion cracking.

Following repository disposal, the canister shell will be enclosed in a disposal overpack that will provide barrier capability and mechanical strength for disposal. After disposal the canister shell is no longer assigned a containment function and can be ignored in disposal performance analyses. However, the basket and neutron absorbers have the important role of limiting the possibility of nuclear criticality in the disposal environment. The time available for corrosion is much longer after disposal, and an important question addressed by this test plan is whether the materials will corrode slowly enough to maintain structural integrity for at least 10,000 years, on exposure to ground water in a breached waste package. We propose to evaluate 304 and 316 SS, but also more corrosion-resistant steels such as super-austenitic, duplex, and super-duplex stainless steels, using both general and localized corrosion monitoring tests to establish corrosion rates and component lifetimes.

Finally, it is unlikely that the aluminum-based neutron absorber materials that are commonly used today will survive for 10,000 years on exposure to ground water, as the aluminum will act as a sacrificial anode for the steel. We propose to test borated and Gd-bearing stainless steels for general and localized corrosion resistance in repository-relevant conditions.

7. REFERENCES

Andersson, J., Ahokas, H., Hudson, J. A., Koskinen, L., Luukkonen, A., Löfman, J., Keto, V., Pitkänen, P., Mattila, J., Ikonen, A. T. K. and Ylä-Mella, M. (2007). *Olkiluoto site description 2006*. POSIVA 2007-03, Olkiluoto: Posiva Oy.

Note: the following list of standards include some that are relevant, but not cited in the text.

ASTM E399. *Standard Test Method for Linear-Elastic Plane-Strain Fracture Toughness K_{Ic} of Metallic Materials.*

ASTM E1304. *Standard Test Method for Plane-Strain (Chevron-Notch) Fracture Toughness of Metallic Materials*

ASTM E1820. *Standard Test Method for Measurement of Fracture Toughness*.

ASTM F1459. *Standard Test Method for Determination of the Susceptibility of Metallic Materials to Hydrogen Gas Embrittlement (HGE).*

ASTM G1. *Standard Practice for Preparing, Cleaning, and Evaluating Corrosion Test Specimens.*

ASTM G5. *Standard Reference Test Method for Making Potentiostatic and Potentiodynamic Anodic Polarization Measurements.*

ASTM G30. *Standard Practice for Making and Using U-Bend Stress-Corrosion Test Specimens.*

ASTM G31. *Standard Guide for Laboratory Immersion Corrosion Testing of Metals.*

ASTM G38. *Standard Practice for Making and Using C-Ring Stress-Corrosion Test Specimens.*

ASTM G39. *Standard Practice for Preparation and Use of Bent-Beam Stress-Corrosion Test Specimens.*

ASTM G46. *Standard Guide for Examination and Evaluation of Pitting Corrosion.*

ASTM G59 *Standard Test Method for Conducting Potentiodynamic Polarization Resistance Measurements.*

ASTM G102. *Standard Practice for Calculation of Corrosion Rates and Related Information from Electrochemical Measurements.*

ASTM G168. *Standard Practice for Making and Using Precracked Double Beam Stress Corrosion Specimens.*

Frape, S., Blyth, A., Blomqvist, R., McNutt, R. and Gascoyne, M. 2003. 5.17 Deep Fluids in the Continents: II. Crystalline Rocks. In: *Treatise on Geochemistry* (Eds. H. Holland, and K. Turekian). pp. 541-580.

Hanson, B., Alsaed, H., Stockman, C., Enos, D., Meyer, R. and Sorenson, K. 2012. *Gap Analysis to Support Extended Storage of Used Nuclear Fuel, FCRD-USED-2011-000136* Rev 0. U.S. Department of Energy, Used Fuel Disposition R&D Campaign.

Hardin, E.L. 2013. *Spent Fuel Canister Disposability Baseline Report*. FCRD-UFD-2013-000330 Rev. 0. U.S. Department of Energy, Office of Used Nuclear Fuel Disposition. December, 2013.

Hardin, E.L., D.J. Clayton, R.L. Howard, J.M. Scaglione, E. Pierce, K. Banerjee, M.D. Voegele, H.R. Greenberg, J. Wen, T.A. Buscheck, J.T. Carter, T. Severynse and W.M. Nutt 2013. *Preliminary Report on Dual-Purpose Canister Disposal Alternatives (FY13).* FCRD-UFD-2013-000171 Rev. 1. U.S. Department of Energy, Office of Used Nuclear Fuel Disposition. August, 2013.

Hardin, E., C. Bryan, A. Ilgen, E. Kalinina, K. Banerjee, J. Clarity, R. Howard, R. Jubin, J. Scaglione, F. Perry, L. Zheng, J. Rutqvist, J. Birkholzer, H. Greenberg, J. Carter and T. Severynse 2014. *Investigations of Dual-Purpose Canister Direct Disposal Feasibility (FY14).* FCRD-UFD-2014-000069 Rev. 1. U.S. Department of Energy, Office of Used Nuclear Fuel Disposition. August, 2014.

Hosford, W.F. 2012. *Iron and Steel*. Cambridge University Press.

Ilgen, A., D. Enos, C. Bryan, R. Rechard and E. Hardin 2014. *Experimental Plan for DPC/Overpack Performance in a Repository*. FCRD-UFD-2014-000596. U.S. Department of Energy, Office of Used Nuclear Fuel Disposition. October, 2014.

Jerden, J., Frey, K., Copple, J. and Ebert, W. 2014. *ANL Mixed Potential Model For Used Fuel Degradation: Application to Argillite and Crystalline Rock Environments*. Argonne National Laboratory, Lemont, IL. 32p.

Kain, R.M. 1990. "Marine Atmospheric Stress Corrosion Cracking of Austenitic Stainless Steels." *Materials Performance* 29(12), 60.

Kursten, B., Smailos, E., Azkarate, I., Werme, L., Smart, N.R. and Santarini, G. 2004. *COBECOMA: State-of-the-art document on the COrrosion BEhaviour of COntainer MAterials. European Commission 5th Euratom Framework Programme, 1998-2002*. Contract no. FIKW-CT-20014-20138 Final Report: European Commission.

Lai, J.K.L., Shek, C.H. and Lo, K.H., 2012. *Stainless Steels: An Introduction and Their Recent Developments*, Bentham e Books.

Lister, T., Mizia, R., Erickson, A. and Birk, S. 2007. *Electrochemical Corrosion Testing of Borated Stainless Steel Alloys*. INL/EXT-07-12633. Idaho National Laboratory, Idaho Falls, ID. 26 p.

Mintz, T. S., Caseres, L., He, X., Dante, J., Oberson, G., Dunn, D. S. and Ahn, T. 2012. "Atmospheric Salt Fog Testing to Evaluate Chloride-Induced Stress Corrosion Cracking of Type 304 Stainless Steel." *Corrosion 2012*: Salt Lake City. March 11-15, NACE.

Mizia R.E., Pinhere, P.J., Dupont, J.N., Robino, C.V. and Lister, T.E. 2001. "Corrosion Performance of a Gadolinium- Containing Stainless Steel." *Corrosion 2001*: Houston, TX. NACE01138.

Nakayama, G. 2006. "Atmospheric stress corrosion cracking (ASCC) susceptibility of stainless alloys for metallic containers." In: VanIseghem, P., ed., *Scientific Basis for Nuclear Waste Management XXIX*. V.932. pp. 845-852.

NIST SOP No. 7. *Recommended Standard Operating Procedure for Weighing by Single Substitution Using a Single-Pan Mechanical Balance, a Full Electronic Balance, or a Balance with Digital Indications and Built-In Weights*.

NRC (U.S. Nuclear Regulatory Commission) 2013. *Finite Element Analysis of Weld Residual Stresses in Austenitic Stainless Steel Dry Cask Storage System Canisters*. NRC Technical Letter Report. U.S. NRC, Washington, DC. 37 pp. (ADAMS ML13330A512).

NRC (U.S. Nuclear Regulatory Commission) 2014. Assessment of Stress Corrosion Cracking Susceptibility for Austenitic Stainless Steels Exposed to Atmospheric Chloride and Non-Chloride Salts. NUREG/CR-7170. U.S. NRC, Washington, DC. 173 pp.

Outokumpu 2013. *Handbook of Stainless Steel*. Outokumpu Stainless AB, Avesta Research Centre, Avesta, Sweden.

Pourbaix, M. 1974. *Atlas of Electrochemical Equilibria in Aqueous Solutions*, NACE International.

Prosek, T., Le Gac, A., Thierry, D., Le Manchet, S., Lojewski, C., Fanica, A., Johansson, E., Canderyd, C., Dupoiron, F., and Snauwaert, T. 2014. "Low temperature stress corrosion cracking of austenitic and duplex stainless steels under chloride deposits." *Corrosion Science*. Published online: June 6, 2014.

Smart, N. R., Blackwood, D. J., Marsh, G. P., Naish, C. C., O'Brien, T. M., Rance, A. P. and Thomas, M. I. 2004. The anaerobic corrosion of carbon and stainless steels in simulated cementitious repository environments: A summary review of NIREX research. AEAT/ERRA-0313, Harwell, England: AEA Technology.

Shirai, K., Tani, J., Arai, T., Wataru, M., Takeda, H., and Saegusa, T. 2011. "SCC evaluation test of a multi-purpose canister." In: *Proceedings of the 13th International High-Level Radioactive Waste Management Conference (IHLRWMC)*. Albuquerque, NM. American Nuclear Society. pp. 824-831.

Tani, J. I., Mayuzurmi, M., and Hara, N. 2009. "Initiation and propagation of stress corrosion cracking of stainless steel canister for concrete cask storage of spent nuclear fuel." *Corrosion*. V.65, N.3. pp. 187-194.

Tani, J., Shirai, K., Wataru, M., Takeda, H., and Saegusa, T. 2010. *Stress Corrosion Cracking of Stainless Steel Canister of Concrete Cask*. Central Research Institute of Electric Power Industry-CRIEPI. Kanagawa, Japan.